

## Eta-Mesic Nucleus: A New Form of Nuclear Matter \*

Q. HAIDER

Physics Department, Fordham University, Bronx, N. Y. 10458

AND

L.C. LIU

Theoretical Division, Los Alamos National Laboratory, Los Alamos, N. M 87545

*(Received November 10, 2018)*

Formation of  $\eta$ -mesic nucleus, a bound state of an  $\eta$  meson in a nucleus, is reviewed in this paper. Three different theoretical approaches are used to calculate the binding energies and widths of such nuclei. The effect of  $\eta$ -mesic nucleus in pion double-charge-exchange reaction is discussed. Experimental efforts by different groups to detect the nucleus are also discussed. The ramifications of the theoretical and experimental studies of the bound state of  $\eta$  in a nucleus are pointed out.

PACS numbers: 24.60.D, 13.75.G, 21.10.D

**1. Introduction**

In the past, bound systems of strongly interacting particles in a nucleus or atom, such as hyperons and mesons, have provided valuable information about various aspects of hadron-nucleon interaction in a many-body environment. For example, experimental and theoretical studies of hypernuclei led to impressive advances in our knowledge of the  $\Lambda N$  and  $\Sigma N$  interactions.

Until recently it was believed that the  $\eta$  meson plays almost no role in nuclear physics because the  $\eta NN$  coupling constant is very small compared to  $\pi NN$  and  $\pi N\Delta$  coupling constants. This is in sharp contrast to  $\pi$ -nucleus interaction which has been studied extensively. The situation has, however, changed recently in medium- and high-energy nuclear reactions where significant amount of pion induced  $\eta$  production has been observed

---

\* Talk presented by Q.H. at the International Symposium on Meson Physics, held 1-4 October, 2008 at Kraków, Poland. All correspondences should be sent to haider@fordham.edu

at pion energies near 500 MeV [1]. In view of this, there has been a surge of interest in studying the  $\eta$  meson within the framework of nuclear physics. Some of the studies have led to interesting surprises, such as the prediction of the existence of a bound state of  $\eta$  meson in a nucleus, termed  $\eta$ -mesic nucleus, and the phenomenon of “mesonic compound nucleus” in high energy pion double-charge-exchange reactions. In this paper, we will describe the formation of the  $\eta$ -mesic nucleus and point out the relevant physics that we can hope to learn by using the  $\eta$  meson as a nuclear probe.

## 2. Formation of Eta-Mesic Nucleus

The existence of  $\eta$ -mesic nucleus was first predicted by us in 1986 [2]. It is a consequence of the attractive interaction between the  $\eta$  meson and all the nucleons in the nucleus. The attractive nature of the interaction follows from the work of Bhalerao and Liu [3] who found, from a detailed coupled-channel analysis of  $\pi N \rightarrow \pi N$ ,  $\pi N \rightarrow \pi\pi N$ , and  $\pi N \rightarrow \eta N$  reactions, that near-threshold  $\eta N$  interaction is attractive.

The binding energy  $\epsilon_\eta$  and width  $\Gamma_\eta$  of the  $\eta$ -mesic nucleus are calculated by solving the momentum-space relativistic three-dimensional integral equation

$$\frac{\mathbf{k}'^2}{2\mu} \psi(\mathbf{k}') + \int d\mathbf{k} \langle \mathbf{k}' | V | \mathbf{k} \rangle \psi(\mathbf{k}) = E\psi(\mathbf{k}') , \quad (1)$$

using the inverse-iteration method of Kwon and Tabakin [4]. Here  $\langle \mathbf{k}' | V | \mathbf{k} \rangle$  are momentum-space matrix elements of the  $\eta$ -nucleus optical potential  $V$ , with  $\mathbf{k}$  and  $\mathbf{k}'$  denoting, respectively, the initial and final  $\eta$ -nucleus relative momenta. The  $\mu$  is the reduced mass of the  $\eta$ -nucleus system and  $E = \epsilon_\eta + i\Gamma_\eta/2 \equiv \kappa^2/2\mu$  is the complex eigenenergy. For bound states, both  $\epsilon_\eta$  and  $\Gamma_\eta$  are negative. Three different theoretical approaches to  $V$  are used to calculate  $E$ , and they are described below.

### 2.1. Covariant $\eta$ -Nucleus Optical Potential

The first-order microscopic  $\eta$ -nucleus optical potential, after using the covariant reduction scheme of Celenza et al. [5], has the form[2, 6]

$$\begin{aligned} \langle \mathbf{k}' | V | \mathbf{k} \rangle = & \sum_j \int d\mathbf{Q} \langle \mathbf{k}', -(\mathbf{k}' + \mathbf{Q}) | t(\sqrt{s_j})_{\eta N \rightarrow \eta N} | \\ & \times | \mathbf{k}, -(\mathbf{k} + \mathbf{Q}) \rangle \phi_j^*(-\mathbf{k}' - \mathbf{Q}) \phi_j(-\mathbf{k} - \mathbf{Q}) , \end{aligned} \quad (2)$$

where the off-shell  $\eta N$  interaction  $t_{\eta N \rightarrow \eta N}$  is weighted by the product of the nuclear wave functions  $\phi_j^* \phi_j$  corresponding to having the nucleon  $j$  at the

Table 1. Binding energies and half-widths (both in MeV) of  $\eta$ -mesic nuclei given by the full off-shell calculation. No bound state solutions were found for  $A \leq 10$ .

Nucleus	Orbital ( $n\ell$ )	$\epsilon_\eta + i\Gamma_\eta/2$
$^{12}\text{C}$	1s	$-(1.19 + 3.67i)$
$^{16}\text{O}$	1s	$-(3.45 + 5.38i)$
$^{26}\text{Mg}$	1s	$-(6.39 + 6.60i)$
$^{40}\text{Ca}$	1s	$-(8.91 + 6.80i)$
$^{90}\text{Zr}$	1s	$-(14.80 + 8.87i)$
$^{208}\text{Pb}$	1p	$-(4.75 + 6.70i)$
	1s	$-(18.46 + 10.11i)$
	2s	$-(2.37 + 5.82i)$
	1p	$-(12.28 + 9.28i)$
	1d	$-(3.99 + 6.90i)$

momenta  $-(\mathbf{k}+\mathbf{Q})$  and  $-(\mathbf{k}'+\mathbf{Q})$  before and after the collision, respectively. The  $\eta$ -nucleus interaction  $V$  is related to the elementary  $\eta N$  process by the kinematical transformations of Liu and Shakin [7]. The  $\eta N$  invariant mass  $\sqrt{s_j}$  in the c.m. frame of the  $\eta$  and the nucleon  $j$  is given by

$$\begin{aligned}
s_j &= [\{W - E_{C,j}(\mathbf{Q})\}^2 - \mathbf{Q}^2] \\
&\simeq \left[ M_\eta + M_N - |\epsilon_j| - \frac{\mathbf{Q}^2}{2M_{C,j}} \left( \frac{M_\eta + M_A}{M_\eta + M_N} \right) \right]^2 \\
&< (M_\eta + M_N)^2,
\end{aligned} \tag{3}$$

where  $\mathbf{Q}$ ,  $E_{C,j}$  and  $M_{C,j}$  are, respectively, the momentum, total energy, and mass of the core nucleus arising from removing a nucleon  $j$  of momentum  $-(\mathbf{k} + \mathbf{Q})$  and binding energy  $|\epsilon_j|$  from the target nucleus having the momentum  $-\mathbf{k}$ . Calculation of  $V$  involves full off-shell kinematics and integration over the Fermi motion variable  $\mathbf{Q}$ . It requires knowledge of the basic  $t_{\eta N \rightarrow \eta N}$  at subthreshold energies [3]. All kinematic quantities are calculated using well-established Lorentz transformations. For near threshold  $\eta N$  interaction, only one resonance of the  $N^*$  isobar has to be considered for each partial wave. They are  $S_{11}$ ,  $P_{11}$ , and  $D_{13}$  resonances. The  $\eta N$  interaction parameters are taken from ref.[3]. Details of the calculation can be found in refs. [2, 6].

The results of the calculation are presented in table 1. The nuclear wave functions in eq.(2) are derived from experimental form factors with the proton finite size corrected for. From the table 1, it can be seen that  $\eta$  can be

bound in nuclei with mass number  $A > 10$ . The  $\eta$ -nucleus interaction is not strong enough to have a bound state in lighter nuclei. This is because there is a reduction in the strength of the  $\eta$ -nucleus interaction at subthreshold energies. The number of nuclear orbitals in which  $\eta$  can be bound increases with increasing mass number.

It should be mentioned that the calculations do not include the effects of Pauli blocking. However, estimates of the blocking using local-density approximation show about 5% reduction in the widths [2]. The calculated widths of  $\eta$ -mesic nuclei vary from 10 to 13 MeV in lighter nuclei and are between 15 and 20 MeV for the heavier ones. About 95% of the width is due to the decay of the  $\eta$ -mesic nucleus with the emission of one pion and one nucleon. The remaining 5% is due to the emission of two pions [8]. As absorptions of  $\eta N \rightarrow N$  and  $\eta NN \rightarrow NN$  are strongly suppressed kinematically, their contributions to the width are insignificant. Widths of the order of keV may be possible if  $\eta NNN \rightarrow NNN$  can take place. In this latter case, the  $\eta$  can then share its energy and momentum with three nucleons.

The binding energy is very sensitive to the  $\eta N$  interaction coupling constant  $g_{\eta NN^*}$ . The value of  $g_{\eta NN^*}$  determined in ref. [3] is 0.77. This leads to a value of 0.28 fm for the real part of the  $s$ -wave  $\eta N$  scattering length  $a_{\eta N}$ , corresponding to an attractive interaction. As an example, it has been shown by Haider and Liu [9] that the bound state of  $\eta$  in  $^{15}\text{O}$  increases with the coupling constant. For  $g_{\eta NN^*} > 0.90$ , however, the binding energy starts to decrease, and then ceases to exist when it becomes greater than 1.0. Furthermore,  $\Re(a_{\eta N})$  also decreases for  $g_{\eta NN^*} > 0.85$  and becomes repulsive at large values.

The existence of at least one bound state of  $\eta$  in medium mass nuclei of radius  $R = r_0 A^{1/3}$  can be understood by considering an equivalent square-well (complex) potential of depth  $V_0 = U_0 + iW_0$ . One  $s$ -wave bound state is possible if the condition

$$\frac{\pi^2}{8\mu} < (|U_0| R^2) < \frac{9\pi^2}{8\mu} \quad (4)$$

is satisfied [10]. In terms of the  $s$ -wave  $\eta N$  scattering length  $a_{\eta N}$ , the condition is

$$X < \Re(a_{\eta N}) < 9X, \quad X = \frac{\pi^2 r_0}{12A^{2/3}} \left(1 + \frac{M_\eta}{M_N}\right)^{-1}, \quad (5)$$

and the potential is given by

$$V_0 = -197.3 \left(\frac{3a_{\eta N}}{2r_0^3}\right) \left(1 + \frac{M_\eta}{M_N}\right) \left(\frac{M_\eta + M_A}{M_\eta M_A}\right). \quad (6)$$

Table 2. Parameters  $X$  and  $9X$  (both in fm) of the equivalent square-well potential calculated with  $a_{\eta N} = (0.28 + 0.19i)$  fm.

Nucleus	$X$	$9X$
$^{12}\text{C}$	0.109	0.981
$^{16}\text{O}$	0.090	0.810
$^{26}\text{Mg}$	0.065	0.585
$^{40}\text{Ca}$	0.048	0.432
$^{90}\text{Zr}$	0.029	0.261
$^{208}\text{Pb}$	0.016	0.144

In the above expression, the masses are in  $\text{fm}^{-1}$  and  $V_0$  is in MeV. The values of  $X$  and  $9X$  are given in table 2 for  $r_0 = 1.1$  fm and  $a_{\eta N} = (0.28 + 0.19i)$  fm [3]. For nuclei with  $A \leq 10$ , one has to use the actual value of  $R$  which is substantially larger than the value given by  $1.1A^{1/3}$  fm. Additionally, the use of equivalent square-well potential and the omission of the imaginary part of the potential break down for lighter nuclei. Consequently, eqs.(4)-(6) should not be applied to nuclei with  $A \leq 10$ . Instead, detailed calculations should be performed. In Zr and Pb,  $\Re(a_{\eta N}) > 9X$ . This explains why there are more than one bound state in these nuclei.

## 2.2. Factorization Approximation

In the factorization approximation (FA), the  $\eta N$  scattering amplitude in eq.(2) is taken out of the  $\mathbf{Q}$  integration and evaluated at a fixed momentum  $\langle \mathbf{Q} \rangle$  given by

$$\langle \mathbf{Q} \rangle = - \left( \frac{A-1}{2A} \right) (\mathbf{k}' - \mathbf{k}) . \quad (7)$$

This choice of  $\langle \mathbf{Q} \rangle$  corresponds to a motionless target nucleon fixed before and after the  $\eta N$  interaction. It has the virtue of preserving the symmetry of the  $t$ -matrix with respect to the interchange of  $\mathbf{k}$  and  $\mathbf{k}'$ . With this approximation, the  $\eta$ -nucleus potential can be written as

$$\begin{aligned} \langle \mathbf{k}' | V_{FA} | \mathbf{k} \rangle &= \langle \mathbf{k}', -(\mathbf{k}' + \langle \mathbf{Q} \rangle) | t(\sqrt{s})_{\eta N \rightarrow \eta N} | \\ &\times | \mathbf{k}, -(\mathbf{k} + \langle \mathbf{Q} \rangle) \rangle f(\mathbf{k}' - \mathbf{k}) , \end{aligned} \quad (8)$$

where

$$f(\mathbf{k}' - \mathbf{k}) = \sum_j \int d\mathbf{Q} \phi_j^*(-\mathbf{k}' - \mathbf{Q}) \phi_j(-\mathbf{k} - \mathbf{Q}) , \quad (9)$$

Table 3. Binding energies and half-widths (both in MeV) of  $\eta$ -mesic nuclei obtained with the factorization approach for different values of the energy shift parameter  $\Delta$  (in MeV).

Nucleus	Orbital ( $n\ell$ )	$\Delta = 0$	$\Delta = 10$	$\Delta = 20$	$\Delta = 30$
<sup>12</sup> C	1s	-(2.18 + 9.96i)	-(1.80 + 6.80i)	-(1.42 + 5.19i)	-(1.10 + 4.10i)
<sup>16</sup> O	1s	-(4.61 + 11.57i)	-(3.92 + 8.13i)	-(3.33 + 6.37i)	-(2.84 + 5.17i)
<sup>20</sup> Ne	1s	-(6.52 + 12.86i)	-(5.63 + 9.16i)	-(4.90 + 7.26i)	-(4.29 + 5.96i)
<sup>24</sup> Mg	1s	-(9.26 + 14.90i)	-(8.09 + 10.75i)	-(7.15 + 8.60i)	-(6.37 + 7.13i)
<sup>26</sup> Mg	1s	-(10.21 + 15.41i)	-(8.95 + 11.17i)	-(7.94 + 8.97i)	-(7.11 + 7.46i)
<sup>28</sup> Si	1s	-(10.84 + 15.70i)	-(9.53 + 11.40i)	-(8.49 + 9.18i)	-(7.62 + 7.65i)
<sup>32</sup> S	1s	-(11.94 + 16.18i)	-(10.56 + 11.80i)	-(9.47 + 9.53i)	-(8.55 + 7.97i)
<sup>40</sup> Ca	1s	-(14.34 + 17.06i)	-(12.75 + 12.55i)	-(11.53 + 10.21i)	-(10.51 + 8.59i)
<sup>46</sup> Ti	1s	-(15.40 + 17.12i)	-(13.73 + 12.66i)	-(12.46 + 10.34i)	-(11.40 + 8.73i)
<sup>52</sup> Cr	1s	-(16.42 + 16.99i)	-(14.65 + 12.63i)	-(13.33 + 10.35i)	-(12.24 + 8.77i)
	1p	-(2.10 + 15.09i)	-(1.40 + 10.54i)	-(0.75 + 8, 21i)	-(0.19 + 6.62i)
<sup>56</sup> Fe	1s	-(16.73 + 16.81i)	-(14.94 + 12.53i)	-(13.60 + 10.28i)	-(12.51 + 8.72i)
	1p	-(2.68 + 15.00i)	-(2.00 + 10.53i)	-(1.34 + 8.25i)	-(0.76 + 6.69i)
<sup>58</sup> Ni	1s	-(17.04 + 16.88)	-(15.23 + 12.59i)	-(13.88 + 10.34i)	-(12.77 + 8.78i)
	1p	-(3.17 + 14.82i)	-(2.43 + 10.47i)	-(1.73 + 8.24i)	-(1.13 + 6.71i)
<sup>70</sup> Zn	1s	-(18.57 + 17.34i)	-(16.62 + 12.98i)	-(15.20 + 10.69i)	-(14.03 + 9.10i)
	1p	-(5.02 + 15.29i)	-(4.20 + 10.94i)	-(3.42 + 8.71i)	-(2.75 + 7.18i)
<sup>90</sup> Zr	1s	-(21.32 + 18.59i)	-(19.15 + 13.97i)	-(17.58 + 11.54i)	-(16.29 + 9.84i)
	1p	-(8.27 + 16.01i)	-(7.19 + 11.47i)	-(6.23 + 9.48i)	-(5.40 + 7.94i)
<sup>208</sup> Pb	1s	-(24.06 + 19.18i)	-(21.88 + 14.44i)	-(20.28 + 11.96)	-(18.96 + 10.22i)
	2s	-(4.89 + 11.04i)	-(3.67 + 8.28i)	-(2.81 + 6.79i)	-(2.12 + 5.72i)
	1p	-(18.33 + 18.97i)	-(16.31 + 14.27i)	-(14.81 + 11.79i)	-(13.56 + 10.06i)
	1d	-(8.27 + 14.07i)	-(6.17 + 10.56i)	-(5.58 + 8.71i)	-(4.66 + 7.41i)

is the nuclear form factor having the normalization  $f(0) = A$ . Guided by the expression for  $\sqrt{s_j}$ , the  $t$ -matrix in eq.(8) is evaluated at  $\sqrt{s} = M_\eta + M_N - \Delta \equiv \sqrt{s_{th}} - \Delta$ , with  $\Delta$  being an energy shift parameter. A downward shift of  $\sim 30$  MeV is used to fit  $\pi N$  scattering data [7].

The bound-state solutions obtained from using the covariant factorized potential with  $\Delta = 0, 10, 20, 30$  MeV are presented in table 3. The interaction parameters used in the FA calculations are same as those used for the off-shell calculations. The nuclear form factors used in the calculations can be found in refs.[11, 12]. A comparison between tables 1 and 3 indicates that the FA results with  $\Delta = 30$  MeV are close to the off-shell results. This indicates that the  $\eta N$  interaction in  $\eta$  bound-state formation takes place at energies 30 MeV below the free-space threshold.

The mass dependence of the 1s binding energies for the  $\Delta = 30$  MeV case is shown in figure 1. The binding energies have been fitted empirically

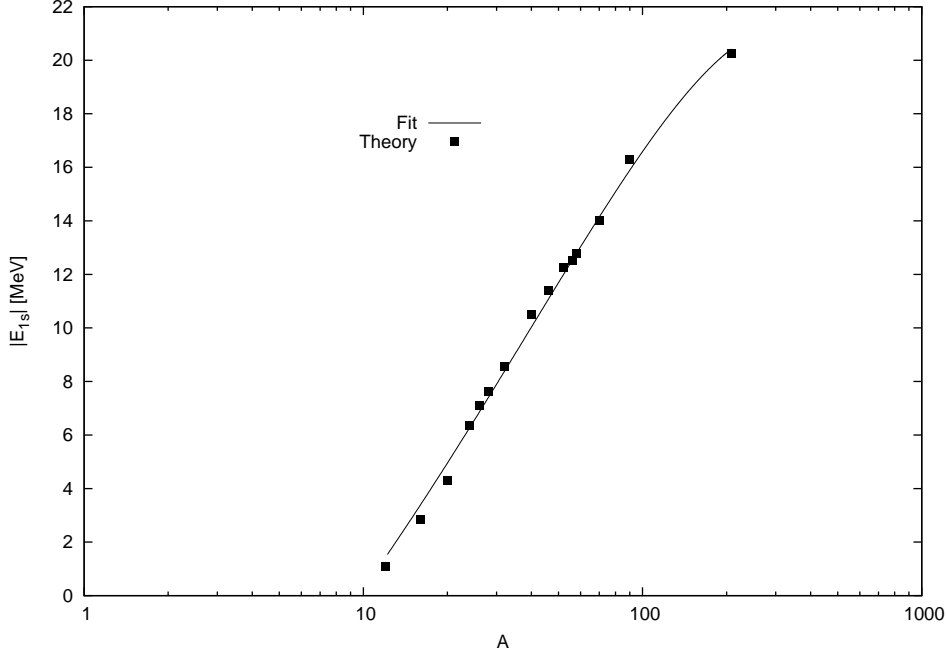


Fig. 1. Dependence of the binding energy of  $\eta$ -mesic nucleus on the mass number  $A$ .

with the formula

$$\epsilon_\eta = aA + bA^{2/3} + cA^{1/3} + d, \quad 12 \leq A \leq 208, \quad (10)$$

where  $a = 0.0003$ ,  $b = -0.9562$ ,  $c = 13.06$ , and  $d = -23.46$  (all in MeV). The above equation resembles the semi-empirical mass formula with  $a$  as the volume energy term and  $b$  as the surface energy term.

### 2.3. On-Shell Optical Potential

First-order low energy  $\eta$ -nucleus on-shell optical potential is

$$\langle \mathbf{k}' | V_{ON} | \mathbf{k} \rangle = -\frac{1}{4\pi^2\mu} \left( 1 + \frac{M_\eta}{M_N} \right) a_{\eta N} f(\mathbf{k}' - \mathbf{k}). \quad (11)$$

As will be seen later,  $V_{ON}$  corresponds to  $V_{FA}$  with no energy shift ( $\Delta = 0$ ) and gives an upper limit to the value of  $\epsilon_\eta$ . The only input for the on-shell calculation is the  $s$ -wave  $\eta N$  scattering length  $a_{\eta N}$ .

The scattering length is not directly measurable and its value is model dependent. Different models predict different values of  $a_{\eta N}$  [6]. The value of  $a_{\eta N}$  in the literature varies from  $0.27 \leq \Re(a_{\eta N}) \leq 1.05$ ,  $0.19 \leq \Im(a_{\eta N}) \leq$

Table 4. Binding energies and half-widths (both in MeV) of  $\eta$ -mesic nuclei (1s state only) given by the on-shell optical potential for two different values of the scattering length  $a_{\eta N}$ . No bound state exists in  ${}^3\text{He}$ .

Nucleus	F.A. ( $\Delta = 0$ )	$a_{\eta N} = (0.28 + 0.19i)$ fm	$a_{\eta N} = (0.51 + 0.21i)$ fm
${}^4\text{He}$	–	–	$-(6.30 + 11.47i)$
${}^6\text{Li}$	–	–	$-(3.47 + 6.79i)$
${}^9\text{Be}$	–	–	$-(13.78 + 12.45i)$
${}^{10}\text{B}$	–	$-(0.93 + 8.70)$	$-(15.85 + 13.05i)$
${}^{11}\text{B}$	–	$-(2.71 + 10.91i)$	$-(20.78 + 15.42i)$
${}^{12}\text{C}$	$-(2.18 + 9.96i)$	$-(2.91 + 10.22i)$	$-(19.61 + 14.20i)$
${}^{16}\text{O}$	$-(4.61 + 11.57i)$	$-(5.42 + 11.43i)$	$-(23.26 + 14.86i)$
${}^{20}\text{Ne}$	$-(6.52 + 12.86i)$	$-(7.44 + 12.61i)$	$-(26.72 + 15.94i)$
${}^{24}\text{Mg}$	$-(9.26 + 14.90i)$	$-(10.34 + 14.40i)$	$-(32.00 + 17.59i)$
${}^{26}\text{Mg}$	$-(10.21 + 15.41i)$	$-(11.24 + 14.76i)$	$-(33.11 + 17.73i)$
${}^{28}\text{Si}$	$-(10.84 + 15.70i)$	$-(11.90 + 15.05i)$	$-(34.06 + 17.96i)$
${}^{32}\text{S}$	$-(11.94 + 16.18i)$	$-(13.10 + 15.61i)$	$-(35.90 + 18.46i)$
${}^{40}\text{Ca}$	$-(14.34 + 17.06i)$	$-(15.46 + 16.66i)$	$-(38.85 + 19.16i)$
${}^{46}\text{Ti}$	$-(15.40 + 17.12i)$	$-(16.50 + 17.07i)$	$-(39.82 + 19.44i)$
${}^{52}\text{Cr}$	$-(16.42 + 16.99i)$	$-(17.46 + 17.45i)$	$-(40.5i + 19.76i)$
${}^{56}\text{Fe}$	$-(16.73 + 16.81i)$	$-(17.76 + 17.52i)$	$-(40.67 + 19.85i)$
${}^{58}\text{Ni}$	$-(17.04 + 16.88i)$	$-(18.09 + 17.67i)$	$-(41.13 + 20.02i)$
${}^{70}\text{Zn}$	$-(18.57 + 17.34i)$	$-(19.63 + 18.47i)$	$-(43.52 + 20.93i)$
${}^{90}\text{Zr}$	$-(21.32 + 18.59i)$	$-(22.41 + 19.97i)$	$-(48.40 + 22.60i)$
${}^{208}\text{Pb}$	$-(24.06 + 19.18i)$	$-(24.55 + 19.57i)$	$-(50.27 + 21.42i)$

0.37. A reason for this large range is unavailability of data on  $\eta N$  elastic scattering, which is essential in determining the value of  $a_{\eta N}$ .

The binding energies and half-widths given by eq.(11) are presented in table 4 for two different values of  $a_{\eta N}$ . The nuclear form factors are the same as those used in the FA calculations. For these two scattering lengths, no bound state can exist in  ${}^3\text{He}$ . Upon comparing the third column of table 4 with the off-shell calculation (table 1), it can be seen that the on-shell approximation predicts more strongly bound  $\eta$ -mesic nuclei. Also, as expected, the on-shell results for  $a_{\eta N} = (0.28 + 0.19i)$  fm are similar to those of FA with  $\Delta = 0$  MeV.



Fig. 2. The calculated energy dependences of the DCX reaction described in the text leading to the double isobaric analog state.

### 3. Eta-Mesic Nucleus and Pion DCX

Eta-mesic nucleus can affect high-energy pion double-charge-exchange (DCX) reactions through the formation of “mesonic compound nucleus” [13]. For pion kinetic energies  $T_\pi > 400$  MeV,  $\eta$  production channel is open in most nuclei. As a result, the DCX reaction can proceed via  $\pi^+ \rightarrow \pi^0 \rightarrow \pi^-$  or  $\pi^+ \rightarrow \eta \rightarrow \pi^-$ . While  $\pi^0$  is in the continuum,  $\eta$  can either be in the continuum or in a nuclear bound state. The DCX amplitudes associated with the  $\eta$ -nucleus bound states, on the other hand, have resonance structure.

The calculated cross sections for the reaction  $^{14}\text{C}(\pi^+, \pi^-)^{14}\text{N}$  as a function of  $T_\pi$  at momentum transfers  $q = 0$  and 210 MeV/c are shown in figure 2. The solid curves represent the contribution from the resonant ampli-

tude associated with the formation of  $\eta$ -mesic nucleus. The dashed curves represent contribution from the nonresonant amplitude only. The interference of these amplitudes is responsible for the presence of narrow resonance structure at  $T_\pi \sim 415$  MeV for  $q = 210$  MeV/c case. The width of the resonance is about 10 MeV, which reflects the width ( $\sim 11$  MeV) of the  $\eta$ -mesic nucleus used in the calculations. The DCX studies, therefore, can be used as an alternative way to determine the width of  $\eta$ -mesic nucleus. Other processes in which one can expect to see these kind of effects is  $(\pi, \pi')$  reactions leading to certain specific final states. The  $\eta$ -nucleus bound state amplitude for these kind of reactions is not small, in comparison to the nonresonant amplitude. The study of the resonance pattern in the energy dependence of the cross section can yield information on the relative phase between resonant and nonresonant amplitudes.

#### 4. Experimental Search for Eta-Mesic Nucleus

Several experiments were performed to detect  $\eta$ -mesic nucleus. The first experiment at Brookhaven National Laboratory [14] in 1987 was based on the work of Liu and Haider [15]. A second experiment, based on the pion DCX calculations [13] was done at LAMPF by Johnson et al. [16]. While these experiments could not confirm unambiguously the existence of  $\eta$ -mesic nucleus, they did not rule out such a possibility either. In recent publications, Sokol et al. [17] claim to have observed  $\eta$ -mesic nucleus in experiments involving photo-mesonic reactions.

Recently, an experiment has been done at Jülich by the COSY-GEM Collaboration [18], making use of the transfer reaction  $p + {}^{27}\text{Al} \rightarrow {}^3\text{He} + {}^{25}\text{Mg}_\eta$ . Analysis of the data clearly indicates the detection of bound state of  $\eta$  in  ${}^{25}\text{Mg}$ . Vigorous efforts are also underway to detect bound state of  $\eta$  in  ${}^3, {}^4\text{He}$ . It is claimed that a “quasibound state” of  $\eta$  in  ${}^3\text{He}$  may have been observed in the  $dp \rightarrow {}^3\text{He}\eta$  reaction [19, 20]. This is in sharp contrast to the findings of the COSY-11 and COSY-at-WASA groups [21], also looking for the bound state of  $\eta$  in  ${}^3\text{He}$  in  $dp$  collisions. Within the statistical sensitivity achieved by them, they could not confirm the existence of  $\eta$ - ${}^3\text{He}$  bound state. This is in agreement with the predictions presented in this paper.

#### 5. Conclusions

The formation of  $\eta$ -mesic nucleus is a natural consequence of the attraction between the  $\eta$  meson and the nucleon at very low energies. However, the attraction is not strong enough to bind an  $\eta$  onto a single nucleon. The bound state formation is possible in a finite nuclei with mass number greater than 10.

The calculated binding energies and widths of  $\eta$ -nucleus bound states strongly depend on the subthreshold dynamics of the  $\eta N$  interaction. The present analysis indicates that the average  $\eta N$  interaction energy in mesic-nucleus formation is below the threshold. What matters for the bound-state formation is not the  $\eta N$  interaction at the threshold but the effective in-medium interaction. Because the subthreshold behavior of  $\eta N$  interaction is very model dependent, it is useful for theorists to publish not only the  $\eta$ -nucleon scattering length  $a_{\eta N}$ , but also the corresponding subthreshold values as a function of the shift parameter  $\Delta$ .

The downward shift in the effective interaction energy can lead to a substantial reduction of the attraction of in-medium  $\eta$ -nucleon interaction with respect to its free-space value. Consequently, predictions based upon using free-space  $\eta N$  scattering length inevitably overestimate the binding of  $\eta$ . One must bear this in mind when using the predictions given by such calculations as guide in searching for  $\eta$ -nucleus bound states.

Recent experimental confirmation [18] of the existence of  $\eta$ -mesic nucleus will enable us to improve upon the existing models or identify additional physics that has to be incorporated in them. Because the binding energies of  $\eta$  meson depend strongly on the coupling between the  $\eta N$  and the  $N^*(1535)$  channels [3], studies of  $\eta$ -mesic nucleus will be able to yield detailed information on the  $\eta NN^*$  coupling constant involving bound nucleons. It can also lead to a new class of nuclear phenomenon,  $\eta$ -mesic compound nucleus resonances. An awareness of this phenomenon could be helpful to the analysis of nuclear reactions at energies above the threshold for  $\eta$  production.

The  $\eta$ -mesic nuclear levels correspond to an excitation energy of  $\sim 540$  MeV, to be compared with an excitation energy of  $\sim 200$  MeV associated with the  $\Lambda$ - and  $\Sigma$ -hypernuclei. The existence of nuclear bound states with such high excitation energies provides the possibility of studying nuclear structure far from equilibrium.

## REFERENCES

- [1] J.C. Peng, *Hadronic Probes and Nuclear Interactions*, AIP Conf. Proc. No. **133**, 255 (1985).
- [2] Q. Haider and L.C. Liu, *Phys. Lett.* **B 172**, 257 (1986); **B 174**, 465E (1986).
- [3] R.S. Bhalerao and L.C. Liu, *Phys. Rev. Lett.* **54**, 865 (1985).
- [4] Y.R. Kwon and F.B. Tabakin, *Phys. Rev.* **C 18**, 932 (1978).
- [5] L.S. Celenza, M.K. Liou, L.C. Liu, and C.M. Shakin, *Phys. Rev.* **C 10**, 398 (1974).
- [6] Q. Haider and L.C. Liu, *Phys. Rev.* **C 66**, 0425208 (2002).
- [7] L.C. Liu and C.M. Shakin, *Prog. Part. and Nucl. Phys.* **5**, 207 (1980).

- [8] Q. Haider and L.C. Liu, *Intersections Between Particle and Nuclear Physics*, AIP Conf. Proc. No. **150**, 930 (1986).
- [9] Q. Haider and L.C. Liu, *Phys. Lett.* **B 209**, 11 (1988).
- [10] L.I. Schiff, *Quantum Mechanics* (3rd ed., Mc-Graw Hill, N.Y., 1968).
- [11] H.R. Collard, L.R.B. Elton, and R. Hofstadter, *Numerical Data and Functional Relationships in Science and Technology*, Vol. 2 Nuclear Radii, edited by H. Schopper (Springer-Verlag, N.Y., 1967).
- [12] C.W. de Jager, H. de Vries, and C. de Vries, *Atomic Data and Nuclear Data Tables* **14**, 479 (1974).
- [13] Q. Haider and L.C. Liu, *Phys. Rev.* **C 36**, 1636 (1987).
- [14] R.E. Chrien et al., *Phys. Rev. Lett.* **60**, 2595 (1988).
- [15] L.C. Liu and Q. Haider, *Phys. Rev.* **C 34**, 1845 (1986).
- [16] J.D. Johnson et al., *Phys. Rev.* **C 47**, 2571 (1993).
- [17] G.A. Sokol et al., *Particles and Nuclei Letters* **5**, 71 (2000); see also *Proceedings of the IX International Seminar on Electromagnetic Interaction of Nuclei at Low and Medium Energies*, Moscow, 2000, p.214.
- [18] A. Budzanowski et al., *Phys. Rev.* **C79**, 012201(R) (2009).
- [19] T. Mersmann et al., *Phys. Rev. Lett.* **98**, 242301 (2007).
- [20] C. Wilkin et al., *Phys. Lett.* **B 654**, 92 (2007).
- [21] J. Smyrski et al., *Phys. Lett.* **B 649**, 258 (2007); *Nucl. Phys.* **A 790**, 438 (2007); *Acta Physica Slovenia* **56**, 213 (2006).